THE JOURNAL OF BIOLOGICAL CHEMISTRY VOL. 291, NO. 7, pp. 3333–3345, February 12, 2016

c-Rel Regulates *Inscuteable* Gene Expression during Mouse Embryonic Stem Cell Differentiation*

Received for publication, July 17, 2015, and in revised form, December 14, 2015 Published, JBC Papers in Press, December 22, 2015, DOI 10.1074/jbc.M115.679563

Riki Ishibashi[‡§], Satoshi Kozuki[‡§], Sachiko Kamakura[¶], Hideki Sumimoto[¶], and Fumiko Toyoshima[‡§1]

From the [‡]Department of Cell Biology, Institute for Virus Research, Kyoto University, Sakyo-ku, Kyoto 606-8507, Japan, the [§]Department of Mammalian Regulatory Networks, Graduate School of Biostudies, Kyoto University, Sakyo-ku, Kyoto 606-8502, Japan, and the [¶]Department of Biochemistry, Kyushu University Graduate School of Medical Sciences, Fukuoka 812-8582, Japan

Inscuteable (Insc) regulates cell fate decisions in several types of stem cells. Although it is recognized that the expression levels of mouse INSC govern the balance between symmetric and asymmetric stem cell division, regulation of mouse *Insc* gene expression remains poorly understood. Here, we showed that mouse *Insc* expression transiently increases at an early stage of differentiation, when mouse embryonic stem (mES) cells differentiate into bipotent mesendoderm capable of producing both endoderm and mesoderm in defined culture conditions. We identified the minimum transcriptional regulatory element (354 bases) that drives mouse *Insc* transcription in mES cells within a region >5 kb upstream of the mouse *Insc* transcription start site. We found that the transcription factor reticuloendotheliosis oncogene (c-Rel) bound to the minimum element and promoted mouse *Insc* expression in mES cells. In addition, short interfering RNA-mediated knockdown of either mouse INSC or c-Rel protein decreased mesodermal cell populations without affecting differentiation into the mesendoderm or endoderm. Furthermore, overexpression of mouse INSC rescued the mesoderm-reduced phenotype induced by knockdown of c-Rel. We propose that regulation of mouse *Insc* expression by c-Rel modulates cell fate decisions during mES cell differentiation.

Insc was first identified as a novel neural precursor gene in *Drosophila* (1). Insc protein expression has been detected in embryonic areas where cell shape changes or movement occurs (*i.e.* neuroectoderm, midgut primordium, and muscle precursors) (1). More precise roles have emerged for Insc protein activity based on studies using neuroblasts, stem cells found in the central nervous system of *Drosophila*, which undergo asymmetric cell division (2–5). In neuroblasts, Insc localizes to the apical cell cortex by directly associating with bazooka-Par6-aPKC cell polarity protein complexes, whereas cell fate determinants, such as miranda (Mira), prospero (Pros), brain tumor (Brat), and Numb, localize to the basal cortex (6–20). Alignment of the mitotic spindle along the apical-basal polarity axis drives asymmetric cell division to produce one self-renewing neuroblast and one ganglion mother cell fated for neural differentiation by asymmetrical inheritance of cell fate determinants (6, 10, 11, 13, 21, 22). Insc plays a critical role in apical-basal spindle positioning by connecting spindle capturing machineries, consisting of partner of inscuteable (Pins) and mushroom body defect (Mud), with apical bazooka-Par6-aPKC cell polarity complexes (23–26).

Similar molecular machineries are conserved in neural progenitors (27, 28) and skin basal cells of mice (29–31), whereby mouse INSC (the mouse homologue of mammalian inscuteable) regulates spindle orientation and cell fate determination together with Par-3 (vertebrate homolog of Bazooka) and LGN (vertebrate counterpart of Pins) (27–31). Previous reports show that ectopic expression of mouse INSC promotes apical-basal spindle positioning in neuronal progenitors and keratinocytes, whereas loss of mouse INSC randomizes or promotes a planar spindle orientation (27–31). Importantly, loss of mouse INSC in radial glia cells decreases neurogenesis, leading to defects in cortical organization, whereas mouse INSC overexpression expands the neuronal cell pool. Therefore, expression levels of mouse INSC appear to be critical for cell fate decision and generation of the correct number of differentiated cells. However, regulation of mouse *Insc* gene expression remains poorly understood, with little information on mouse *Insc* promoters. One reason for this gap in knowledge is the lack of established approaches to investigate regulation of mouse *Insc* gene expression during mammalian cell differentiation.

Embryonic stem (ES)[2] cells are pluripotent and can be differentiated into all cell types found throughout the body (32–35). Here, we demonstrate that expression of mouse INSC transiently increases during mouse ES (mES) cell differentiation into bipotent mesendoderm cells capable of giving rise to both endoderm and mesoderm lineages in defined culture conditions (36, 37). In this system, we identified DNA regulatory elements involved in mouse *Insc* gene expression, which are located more than 5 kb upstream of the mouse *Insc* transcription start site (TSS). We specified the minimum transcription-promoting sequences and identified c-Rel as a key transcription factor that drives mouse *Insc* expression in mES cells. Knockdown of mouse INSC or c-Rel protein leads to a decrease in the proportion of mesoderm cells without alterations in mesendo-

* This work was supported by grants from the Funding Program for Next Generation World-Leading Researchers (Grant LS069 to F. T.), the Naito Foundation (to F. T.), and the Platform Project for Dynamic Approaches to Living System from the Japan Agency for Medical Research and Development (to A. M. E. D.). The authors declare that they have no conflicts of interest with the contents of this article.

[1] To whom correspondence should be addressed: Dept. of Cell Biology, Institute for Virus Research, Kyoto University, Sakyo-ku, Kyoto 606-8507, Japan. Tel.: 81-75-751-4015; Fax: 81-75-751-4037; E-mail: ftoyoshi@virus.kyoto-u.ac.jp.

[2] The abbreviations used are: ES, embryonic stem; mES, mouse ES; VEGFR, vascular endothelial growth factor receptor; TSS, transcription start site; qPCR, quantitative PCR; Tg, transgenic.

derm and endoderm cells, indicating a requirement for mouse INSC in the mesoderm cell fate decision. Our results provide further supporting evidence for how c-Rel regulates mesoderm differentiation by promoting mouse *Insc* expression. This study demonstrates for the first time that the c-Rel/mouse INSC axis regulates mesoderm cell fate decision during mES cell differentiation.

Experimental Procedures

Cell Culture—All cell culture products, unless noted otherwise, were Gibco brand purchased from Life Technologies. Goosecoid (Gsc)$^{gfp/+}$ ES cells were maintained on gelatin-coated dishes in Glasgow minimum essential medium supplemented with 1% fetal calf serum (FCS), 10% KnockOut^{TM} serum replacement, 0.1 mM nonessential amino acids, 1 mM sodium pyruvate, 0.1 mM 2-mercaptoethanol, and 1 μl/ml leukemia inhibitory factor (Wako Chemicals). Gsc$^{gfp/+}$ ES/mouse INSC-mCherry and Gsc$^{gfp/+}$ ES/mCherry cells were maintained on gelatin-coated dishes in Glasgow minimum essential medium supplemented with 1% FCS, 10% KnockOut^{TM} serum replacement, 0.1 mM nonessential amino acids, 1 mM sodium pyruvate, 0.1 mM 2-mercaptoethanol, 1 μl/ml leukemia inhibitory factor, and 100 μg/ml Geneticin (Nakarai). For mesendoderm induction, ES cells were seeded onto type IV collagen-coated dishes at a density of 1×10^4 cells/ml in SF-O3 medium (Sanko Junyaku) containing 0.1% bovine serum albumin (BSA; Sigma-Aldrich), 50 μM 2-mercaptoethanol, and 10 ng/ml activin A (R&D Systems). HEK293T cells were cultured in Dulbecco's modified Eagle's medium with 10% FCS.

Western Blotting and Immunoprecipitation—Cells were lysed in lysis buffer (50 mM Tris-HCl, pH 8.0, 150 mM NaCl, 1% Nonidet P-40, 2 mM EGTA, 2 mM $MgCl_2$, 2 mM dithiothreitol (DTT), 1 mM phenylmethylsulfonyl fluoride, 1 mM Na_3VO_4, and 20 μg/ml aprotinin) and centrifuged at 13,000 rpm at 4 °C for 15 min. Supernatants were subjected to Western blotting. Primary antibodies were mouse monoclonal anti-FLAG (F3165, Sigma-Aldrich), rabbit polyclonal anti-Eomes (ab23345, Abcam), goat polyclonal anti-Foxa-2 (sc-9187, Santa Cruz Biotechnology), rabbit polyclonal anti-T-bra (sc-20109, Santa Cruz Biotechnology), mouse polyclonal anti-Par-3 (07-330, Millipore), rabbit anti-LGN (a gift from Dr. Matsuzaki (Riken CDB), rabbit monoclonal anti-Elk1 (E277, Abcam), rabbit monoclonal anti-Ets1 (14069, CST), rabbit polyclonal anti-cRel (sc-71, Santa Cruz Biotechnology), rabbit polyclonal anti-DsRed (632496, Clontech), and mouse monoclonal anti-α-tubulin (T6199, Sigma-Aldrich). An anti-mouse INSC antibody was prepared as described previously (38). Primary antibodies were detected with horseradish peroxidase-conjugated secondary antibodies (GE Healthcare) using Western Lightning® ECL reagents (PerkinElmer Life Sciences) according to the manufacturer's instructions. For immunoprecipitation of mouse INSC-mCherry, cells were lysed in lysis buffer B (50 mM Hepes, pH 7.5, 2 mM EGTA, 2 mM $MgCl_2$, 12.5 mM β-glycerophosphate, 50 mM NaCl, 10% glycerol, 0.5% Nonidet P-40, 10 mM NaF, 1 mM DTT, 1 mM phenylmethylsulfonyl fluoride, 1 mM Na_3VO_4, 2 μg/ml aprotinin, and 1 μg/ml leupeptin) and centrifuged at 15,000 rpm for 15 min at 4 °C. The mouse anti-mCherry antibody (4 μg) was added to the supernatant, followed by incubation at 4 °C for 1 h. Protein A- or G-Sepharose beads (GE Healthcare), preincubated with 3% BSA-PBS, were added to the mixtures, followed by incubation at 4 °C for 2–3 h, and then washed three times with wash buffer (50 mM Hepes, pH 7.5, 2 mM EGTA, 2 mM $MgCl_2$, 12.5 mM β-glycerophosphate, 150 mM NaCl, 0.5% Nonidet P-40, 10 mM NaF, 1 mM DTT, 1 mM phenylmethylsulfonyl fluoride, 1 mM Na_3VO_4, 2 μg/ml aprotinin, and 1 μg/ml leupeptin) and subjected to Western blotting.

TABLE 1
RT-PCR, qPCR and ChIP-PCR primer sets and siRNA sequences
Lowercase letters indicate overhang sequences.

primer	forward primer (5'-3')	reverse primer (5'-3')
Goosecoid	CCAGCAGTGCTCCTGCGTCC	CGACAGCGTGCCCACGTTCA
Eomesodermin	CGGCAAAGCGGACAATAACA	ATGTGCAGCCTCGGTTGGTA
FoxA2	CATCCGACTGGAGCAGCTA	TGTGTTCATGCCATTCATCC
T-brachyury	CTCTAATGTCCTCCCTTGTTGCC	TGCAGATTGTCTTTGGCTACTTTG
Sox17	CGAGCCAAAGCGGAGTCTC	TGCCAAGGTCAACGCCTTC
Vegfr2	ACGTCGACATAGCCTCCACTGTTT	TTCTCGGTGATGTACACGATGCCA
Oct3/4	TCTTTCCACCAGGCCCCCGGCTC	TGCGGGCGGACATGGGGAGATCC
Nanog	AGGGTCTGCTACTGAGATGCT	CAACACCTGGTTTTTCTGCCACCG
Inscuteable	GTGGGGTTGTAGCCCTCTTC	CACAGGATACCGTCCACCTTC
LGN	TCTGCTGCAAAGAGATCCAAACA	TCCCCCAACACAGATGAGTTCTT
Par3	AGCCTTCTGGTCTTTCGTCA	GGGTGTGAGAACAACGTCCT
Oct1	AGCTCTTGCTTCTAGTGGCTC	CTGGCTGTAGGTGCAGAGTTC
Elk1	TCCTGGACCTCACGGGATG	GGGTAGGACACAAACTTGTAGAC
c-Ets-1	TCCTATCAGCTCGGAAGAACTC	TCTTGCTTGATGGCAAAGTAGTC
c-Rel	ACAACAACCGGACATACCCG	GGTCTGCGTTCTGGTCCAA
Firefly luciferase	GGCTACGTTAACAACCCCGA	TCCACGATCTCCTTCTCGGT
Renilla luciferase	GTCGTCCAACATTATCATGGCC	GAGAACTCGCTCAACGAACGAT
ChIP primer	GGGGTACCTTCCTAAGTGTAATTC	CTAGCTAGCGAGCTTACAGCATGG
G3pdh	ACAGTCCATGCCATCACTGCC	GCCTGCTTCACCACCTTCTTG

siRNA	Sense (5'-3')
Oct3/4	GGA GUC CCA GGA CAU GAA Att
mInsc-1	GCU GGU GGA UUC CUU CUU Att
mInsc-2	CUU CUA CAG UUG AAU GCA Att
Par-3	AGA CAG ACU GGU AGC AGU Att
LGN	UUU AGC UUG AGA GCG UAA GAU GAG G
Luciferase	CUU ACG CUG AGU ACU UCG Att

PCR, RT-PCR, and Quantitative RT-PCR—Total DNA was isolated using phenol/chloroform and ethanol and then subjected to genomic PCR. Total RNA was isolated using an RNeasy® minikit (Qiagen) according to the manufacturer's protocol. First-strand cDNA was synthesized using Moloney murine leukemia virus reverse transcriptase (Life Technologies, Inc.) and random primers (Takara) for quantitative RT-PCR and RT-PCR. Quantitative RT-PCR was performed with KAPA^{TM} SYBR® Fast qPCR Master Mix (KAPA Biosystems) on an ABI7500 cycler (Applied Biosystems). *G3pdh* was used as an internal control. Genomic PCR and RT-PCR were performed with *Taq* DNA polymerase (Life Technologies) on a Veriti® 96-well thermal cycler (Applied Biosystems). Primers used for analyses are shown in Table 1.

siRNA Knockdown—siRNA sequences against Oct3/4, mouse INSC, Par-3, LGN, and luciferase are shown in Table 1. siRNAs targeting mouse Elk1, c-Ets-1, and c-Rel were purchased from Qiagen. Cells were transfected with siRNA using Lipofectamine® 2000 (Life Technologies). Expression levels were analyzed by quantitative RT-PCR.

Mouse Insc Gene Promoter Assay—A series of genomic regions upstream of the mouse *Insc* locus TSS (−5,382, −4,382, −3,382, −2,382, −1,382, −382, and +1 to + 200) were amplified by PCR and cloned into pGL4.10 (Promega). ES cells were transfected with plasmids using Lipofectamine® 2000. Prior to the luciferase assay, cells were treated for 24 h with IKK inhibitor II, wedelolactone (Calbiochem). The luciferase assay was

performed using the Dual-Luciferase® reporter assay system (Promega). Firefly luciferase activity was normalized to control *Renilla* luciferase activity.

Flow Cytometric Analysis—Cells were incubated in cell dissociation buffer (Gibco) and then stained with allophycocyanin-conjugated Avas12 (anti-VEGFR-2) (Biolegend). Stained cells were analyzed using a FACSCantoII™ (BD Biosciences). Dead cells stained with propidium iodide (BD Biosciences) were excluded from analysis.

Cell Staining—Cells were fixed with 4% paraformaldehyde at 37 °C for 10 min, followed by incubation with 0.5% Triton X-100 at room temperature for 10 min. Cells were blocked in 3% BSA (Sigma-Aldrich) at 37 °C for 30 min and then incubated with goat anti-Sox17 (R&D Systems), anti-VEGFR-2, anti-GFP (MBL International), anti-Oct4 (Cell Signaling Technology), and anti-Nanog (BD Bioscience) antibodies at 4 °C overnight. The cells were then washed and incubated for 1 h with appropriate secondary antibodies, including Alexa Fluor® 488-goat anti-rabbit IgG, 546-goat anti-rat IgG, or 647-donkey anti-goat IgG (A11008, A11081, and A21447, respectively; Life Technologies).

Chromatin Immunoprecipitation (ChIP)—Lysates prepared from ES cells transfected with the pGL4.10 reporter plasmid encoding the −5,382 to +200 base genomic region of the mouse *Insc* TSS were cross-linked with 1% formaldehyde at room temperature for 10 min. Glycine was added at a final concentration of 0.125 M, followed by incubation for 10 min at room temperature. The sample was washed once with wash buffer (2% BSA and 0.05% NaN_3 in PBS), the supernatant was removed, and then the pellet was lysed with SDS lysis buffer (50 mM Tris, 10 mM EDTA, 1% SDS, 1 mM phenylmethylsulfonyl fluoride, 1 μg/ml aprotinin, and 1 μg/ml leupeptin) on ice at 10 min. Samples were sonicated on ice, centrifuged at 15,000 rpm at 4 °C for 10 min, and then diluted with ChIP dilution buffer (50 mM Tris, 167 mM NaCl, 1.1% Triton X-100, 0.11% sodium deoxycholate, 1 mM phenylmethylsulfonyl fluoride, 1 μg/ml aprotinin, and 1 μg/ml leupeptin). Rabbit anti-Elk1, c-Ets-1, or cRel antibodies (4 μg) were added to the samples, followed by incubation at 4 °C for 1 h. Protein A-Sepharose/salmon sperm DNA mixtures (50% slurry; Millipore) were preincubated with 3% BSA-PBS at 4 °C for 2–3 h and then added to the samples, followed by incubation at 4 °C overnight. The immunoprecipitates were washed sequentially with wash buffer A (50 mM Tris, 150 mM NaCl, 1 mM EDTA, 1% Triton X-100, 0.1% SDS, and 0.1% sodium deoxycholate), wash buffer B (50 mM Tris, 500 mM NaCl, 1 mM EDTA, 1% Triton X-100, 0.1% SDS, and 0.1% sodium deoxycholate), and wash buffer C (10 mM Tris, 0.25 M LiCl, 1 mM EDTA, 0.5% Nonidet P-40, and 0.5% sodium deoxycholate). The beads were washed twice with Tris-EDTA buffer, and bound DNA was eluted with ChIP elution buffer (10 mM Tris, 300 mM NaCl, 5 mM EDTA, and 0.5% SDS) at 65 °C overnight. Eluted DNA was purified with phenol/chloroform and ethanol and then subjected to qPCR analysis. qPCR was performed with KAPA™ SYBR® Fast qPCR Master Mix (KAPA Biosystems) on an ABI7500 Cycler (Applied Biosystems) using the following primers: GGGGTACCTTCCTAAGTGTAATTC and CTAGCTAGCGAGCTTACAGCATGG.

Results

ES Cell Differentiation into Mesoderm and Endoderm—Previous reports have demonstrated that mES cells differentiate into bipotent mesendoderm cells capable of further differentiation into mesoderm and endoderm lineages under defined culture conditions (Fig. 1*A*) (36, 37). Accordingly, we cultured ES cells harboring a *Gsc-gfp* transgene ($Gsc^{gfp/+}$ ES cells) to monitor mesendoderm differentiation on collagen IV-coated dishes in SF-O3 serum-free medium containing 10 ng/ml activin A. Consistent with previous studies, after 4 days of differentiation, about 50% of the ES cells became positive for Gsc-GFP (Fig. 1*B*). Furthermore, they expressed either vascular endothelial growth factor receptor-2 (VEGFR-2), a mesoderm marker (39), or SRY-box 17 (Sox17), an endoderm marker (40, 41) (Fig. 1*C*). Next, we examined the expression profiles of differentiation marker genes every 24 h. Preceding expression of *Gsc*, eomesodermin (*Eomes*), a mesendoderm marker (36, 37, 42, 43), was expressed at differentiation day 3 (Fig. 1*G*). Expression of forkhead box protein A2 (FoxA2) and T-brachyury (T-bra), mesendoderm genes downstream of *Gsc* and/or *Eomes* (42, 44, 45), and *Sox17* and *VEGFR-2*, respective markers of definitive endoderm and mesoderm (39–41), was increased drastically at differentiation day 4 (Fig. 1*G*). The expression of pluripotency gene *Nanog* (46, 47) decreased rapidly at differentiation day 2, whereas another pluripotency gene, POU domain class 5 transcription factor 1 (*Oct3/4*) (46, 47), decreased gradually until day 4 (Fig. 1*G*), which was consistent with previous reports indicating sustained expression of Oct3/4 during mesoderm/endoderm differentiation (47). The expression profiles of each protein were confirmed by immunostaining of Gsc-gfp, VEGFR-2, Sox17, Nanog, and Oct4 or immunoblotting of Eomes, Foxa2, and T-bra (Fig. 1, *C–F* and *H*). Under this condition, we next examined the expression profiles of *Par-3*, *LGN*, and mouse *Insc*. In ES cells, we detected 3 variants of Par-3 protein by immunoblotting, all of which were down-regulated by RNA interference (RNAi)-mediated knockdown of Par-3 (see Fig. 5*H*, right). During ES cell differentiation, the expression profiles of these Par-3 proteins varied (Fig. 1*J*), whereas expression of *Par-3* mRNA, which was detected using primers in the sequence conserved among the Par-3 transcription variants, increased gradually over time (Fig. 1*I*). Expression levels of *LGN* mRNA and protein were slightly decreased at differentiation day 2 and then increased again to the levels in undifferentiated ES cells (Fig. 1, *I* and *J*). Interestingly, mouse *Insc* mRNA expression was rapidly up-regulated at differentiation day 2 before returning to basal levels at day 3 (Fig. 1*I*), followed by an increase in the mouse INSC protein level at days 2 and 3, and then returning to basal levels at day 4 (Fig. 1*J*). We detected up-regulation of mouse *Insc* mRNA expression even at differentiation day 1 (data not shown). These results prompted us to investigate the transcriptional regulation of the mouse *Insc* gene during ES cell differentiation into mesoderm and endoderm.

Identification of the DNA Regulatory Elements for Mouse Insc Gene Expression—We attempted to identify DNA regulatory elements capable of promoting mouse *Insc* gene transcription. A luciferase assay vector was constructed, in which a region

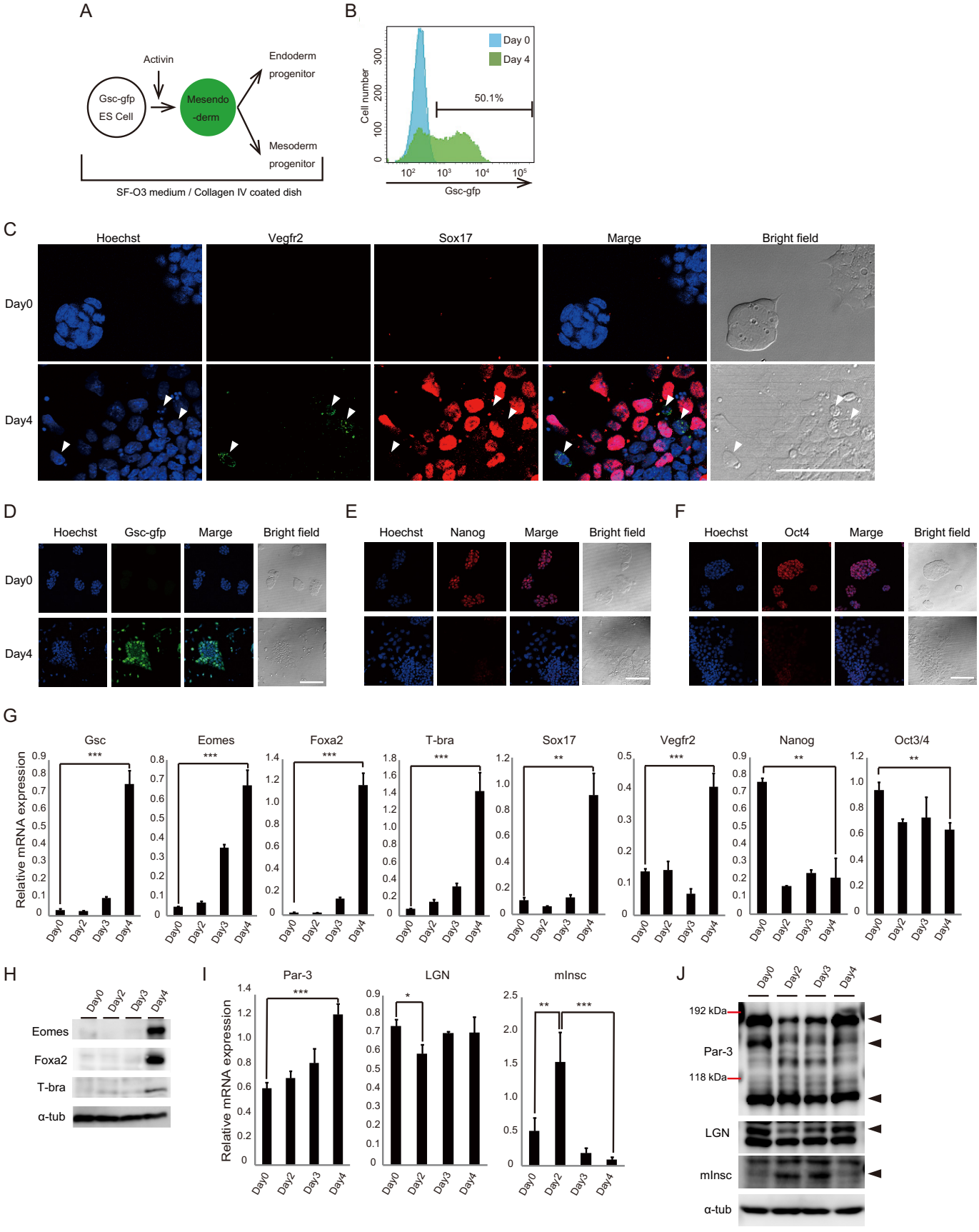
A
Activin
Gsc-gfp
ES Cell
Mesendo
-derm
Endoderm
progenitor
Mesoderm
progenitor
SF-O3 medium / Collagen IV coated dish
B
Day 0
Day 4
50.1%
Cell number
Gsc-gfp
C
Hoechst
Vegfr2
Sox17
Marge
Bright field
Day0
Day4
D
Hoechst
Gsc-gfp
Marge
Bright field
E
Hoechst
Nanog
Marge
Bright field
F
Hoechst
Oct4
Marge
Bright field
G
Gsc
Eomes
Foxa2
T-bra
Sox17
Vegfr2
Nanog
Oct3/4
Relative mRNA expression
H
Eomes
Foxa2
T-bra
α-tub
I
Par-3
LGN
mInsc
Relative mRNA expression
J
192 kDa
Par-3
118 kDa
LGN
mInsc
α-tub

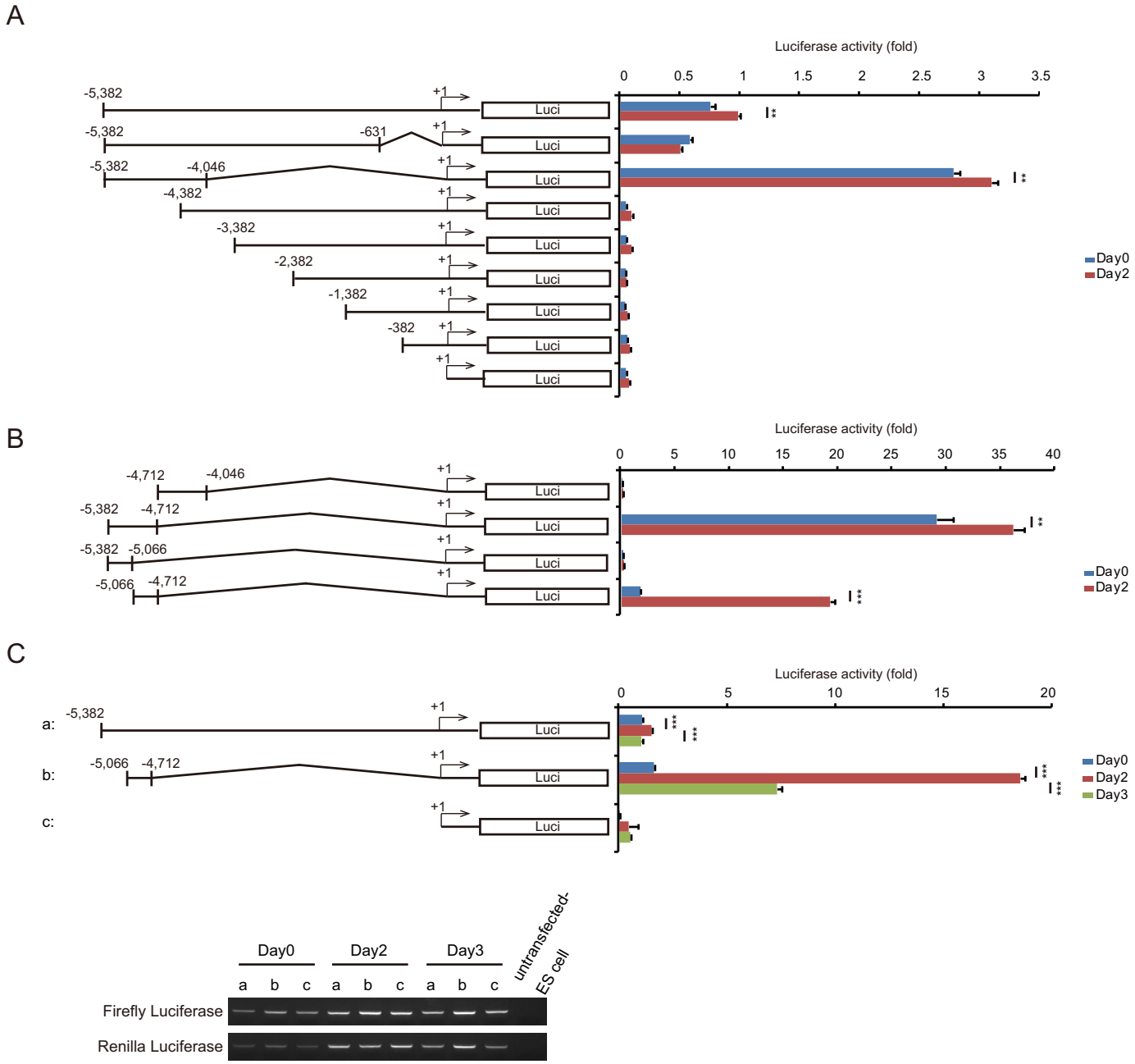

FIGURE 2. **Identification of the DNA element that promotes mouse *Insc* transcription.** *A–C*, ES cells were transfected with luciferase reporter plasmids containing the indicated genomic regions upstream of the mouse inscuteable gene locus together with the control pRL-SV40 plasmid. Luciferase activity was measured at differentiation day 0, 2, or 3. Values are normalized to the activity of co-transfected *Renilla* luciferase (mean ± S.D. (*error bars*) from three experiments; **, $p < 0.01$; ***, $p < 0.001$ analyzed by Dunnett's multiple-comparison test). *Bottom*, PCR analysis for Firefly luciferase and *Renilla* luciferase genes in ES cells in *C* or control untransfected cells, showing the presence of each transfected plasmid.

located −5,382 bases upstream of the mouse *Insc* gene locus was fused to the luciferase-coding sequence. We successfully detected transcription-promoting activity in ES cells (Fig. 2*A*). It is worth noting that this activity was significantly higher after 2 days of differentiation compared with that in undifferentiated ES cells. Furthermore, the transcriptional activity was de-

FIGURE 1. **Mouse INSC is transiently expressed during ES cell differentiation into mesoderm and endoderm.** *A*, culture condition for differentiation of ES cells into mesoderm and endoderm through a bipotent mesendoderm state. *B*, FACS analysis for detecting Gsc-gfp expression after 4 days of differentiation. *C*, immunofluorescence images of Hoechst (*blue*), VEGFR-2 (*green*), and Sox17 (*red*) of mES cells at differentiation days 0 (*top*) and 4 (*bottom*). *Arrowheads*, Vegfr2-positive cells. *Scale bars*, 75 μm. *D–F*, immunofluorescence images of Hoechst (*blue*) and the indicated proteins (Gsc-gfp (*green*) (*D*), Nanog (*red*) (*E*), and Oct4 (*red*) (*F*)) of mES cells at differentiation days 0 (*top*) and 4 (*bottom*). *Scale bars*, 75 μm. *G*, qPCR analysis for mRNA expression of the indicated genes at differentiation days 0, 2, 3, and 4. *H*, Western blotting analysis for Eomes, Foxa2, T-bra, and control α-tubulin proteins in ES cells at differentiation days 0, 2, 3, and 4. *I*, qPCR analysis for expression of *Par-3*, *LGN*, and mouse *Insc* at differentiation days 0, 2, 3, and 4. *J*, Western blotting analysis for Par-3, LGN, mouse INSC, and control α-tubulin proteins in ES cells at differentiation days 0, 2, 3, and 4. *Arrowheads* show each indicated protein. In all qPCR analysis, values are normalized to expression of *G3pdh* (mean ± S.D. (*error bars*) from three experiments). *, $p < 0.05$; **, $p < 0.01$; ***, $p < 0.001$ analyzed by Dunnett's multiple-comparison test.

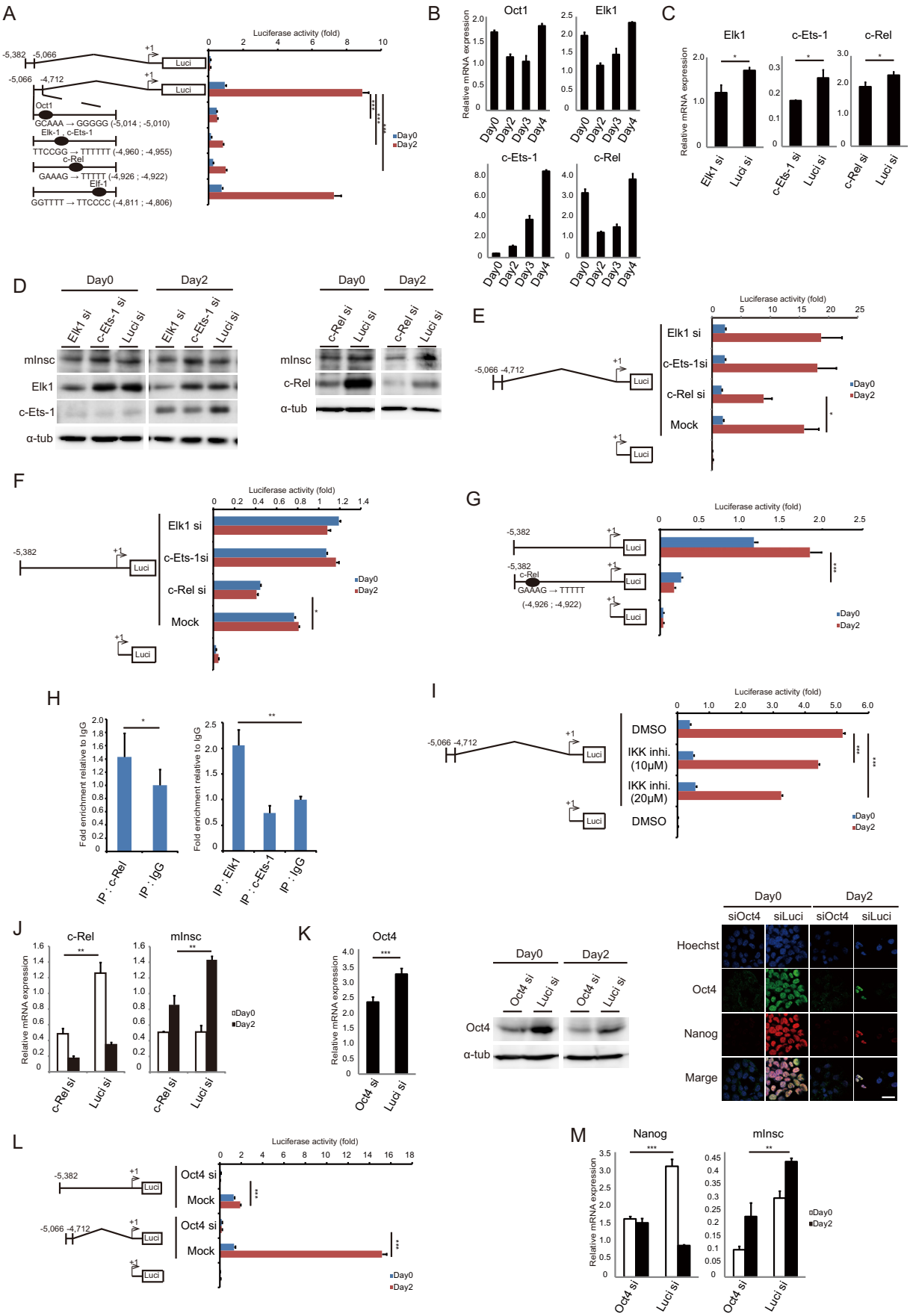
A
Luciferase activity (fold)
-5,382 -5,066
-5,066 -4,712
Oct1
GCAAA → GGGGG (-5,014 ; -5,010)
Elk-1 c-Ets-1
TTCCGG → TTTTTT (-4,960 ; -4,955)
c-Rel
GAAAG → TTTTT (-4,926 ; -4,922)
Elf-1
GGTTTT → TTCCCC (-4,811 ; -4,806)
Luci
Day0
Day2
B
Oct1
Elk1
c-Ets-1
c-Rel
Relative mRNA expression
Day0 Day2 Day3 Day4
C
Elk1
c-Ets-1
c-Rel
Relative mRNA expression
Elk1 si
Luci si
c-Ets-1 si
c-Rel si
D
Day0
Day2
Elk1 si
c-Ets-1 si
Luci si
c-Rel si
mInsc
Elk1
c-Ets-1
c-Rel
α-tub
E
Luciferase activity (fold)
-5,066 -4,712
Elk1 si
c-Ets-1si
c-Rel si
Mock
F
Luciferase activity (fold)
-5,382
G
Luciferase activity (fold)
-5,382
-5,382 c-Rel
GAAAG → TTTTT
(-4,926 ; -4,922)
H
Fold enrichment relative to IgG
IP : c-Rel
IP : IgG
IP : Elk1
IP : c-Ets-1
I
Luciferase activity (fold)
-5,066 -4,712
DMSO
IKK inhi. (10μM)
IKK inhi. (20μM)
J
c-Rel
mInsc
Relative mRNA expression
K
Oct4
Relative mRNA expression
Oct4 si
Luci si
Hoechst
Oct4
Nanog
Marge
siOct4
siLuci
L
Luciferase activity (fold)
-5,382
-5,066 -4,712
Oct4 si
Mock
M
Nanog
mInsc
Relative mRNA expression

creased at differentiation day 3 (Fig. 2*C*, *top*, *a*), reflecting endogenous expression patterns of the mouse *Insc* gene (see Fig. 1*I*). PCR analysis confirmed the presence of each transfected plasmid, even at day 3, excluding the possibility that the decline in luciferase activity at day 3 was due to the loss of the transfected plasmids (Fig. 2*C*, *bottom*, *a*). Similar results were obtained when a region at −6,382 bases upstream of the mouse *Insc* locus was fused to the luciferase-coding sequence (data not shown). Deletion from −631 to −1 bases upstream slightly decreased the transcription-promoting activity (Fig. 2*A*). Interestingly, deletion from −4046 to −1 bases upstream resulted in even stronger transcription-promoting activity (Fig. 2*A*). In addition, a series of 5′-deletion constructs indicated that deletion of bases −5382 to −4382 diminished almost all transcriptional activity (Fig. 2*A*). These data indicate that transcription-promoting elements are located between bases −5382 and −4046 upstream of the mouse *Insc* gene locus. Furthermore, a series of additional deletion constructs revealed a minimum transcription-promoting element between −5066 and −4712 bases upstream (Fig. 2*B*). Promoter activity of this minimum element increased significantly at day 2 but decreased on differentiation day 3 without loss of the transfected plasmids (Fig. 2*C*, *top* and *bottom*, *b*). It is worth noting that the region between −5382 and −4712 bases upstream of the mouse *Insc* gene locus displayed higher transcription-promoting activity than the minimum element (Fig. 2*B*), suggesting the existence of co-regulatory elements that enhance the transcription-promoting activity of the minimum element within the region between −5382 and −5066 bases upstream.

c-Rel Regulates Mouse Insc Gene Expression—Within the minimum transcription-promoting element (−5066 to −4712), we used the Match program of TRANSFAC® version 6.0 to identify putative binding sites for five transcription factors, including POU domain class 2 transcription factor 1 (Oct1), ELK1 member of the ETS oncogene family (Elk1), E26 avian leukemia oncogene 1, 5′ domain (c-Ets-1), c-Rel, and E74-like factor 1 (Elf-1) (Fig. 3*A*, *left*). Next, we inserted a mutation into each transcription factor-binding site and measured the promoter activity. Disruption of Oct1-, Elk1/c-Ets-1-, or c-Rel-biding sites, but not the Elf-1-binding site, resulted in loss of promoter activity (Fig. 3*A*, *right*). This result suggests the possibility that mouse *Insc* gene expression is up-regulated by Oct1, Elk1, c-Ets-1, or c-Rel. Expression levels of *Oct1*, *Elk1*, and *c-Rel* were decreased slightly at differentiation day 2 and then increased again to the levels in undifferentiated ES cells at day 4, whereas the expression level of *c-Ets-1* increased gradually over time (Fig. 3*B*). Thus, we next examined knockdown of each transcription factor by RNAi. Although we were unable to successfully down-regulate expression of Oct1, expression levels of *Elk-1*, *c-Ets-1*, and *c-Rel* were decreased significantly by siRNA in ES cells (Fig. 3*C*). siRNA-mediated knockdown of each protein was confirmed by immunoblotting (Fig. 3*D*). We found that siRNA-mediated knockdown of c-Rel, but not Elk1 or c-Ets-1, significantly decreased promoter activity of both the minimum DNA regulatory element (Fig. 3*E*) and the base −5382 upstream region of the mouse *Insc* locus (Fig. 3*F*). Disruption of the c-Rel-binding site in the base −5382 upstream region of the mouse *Insc* locus significantly decreased its promoter activity (Fig. 3*G*). Moreover, ChIP-qPCR analysis showed binding of endogenous c-Rel protein to the minimum DNA regulatory element (Fig. 3*H*, *left*). We also detected binding of Elk1, but not c-Ets1, to the minimum DNA regulatory element (Fig. 3*H*, *right*). c-Rel belongs to the NF-κB family of transcription factors. Our data showed that treatment of the cells with IKK inhibitor II, wedelolactone, to suppress NF-κB-mediated gene transcription (48) significantly decreased pro-

FIGURE 3. **c-Rel promotes mouse *Insc* transcription.** *A*, putative transcription factor-binding sites in the region between −5,066 and −4,712 upstream of the mouse *Insc* gene locus were identified by the Match program of TRANSFAC® version 6.0. (*left*). ES cells were transfected with luciferase reporter plasmids containing the −5,066 to −4,712 genomic region with each indicated mutation together with control pRL-SV40 plasmid. Luciferase activity was measured at differentiation days 0 and 2. Values are normalized to the activity of co-transfected *Renilla* luciferase (mean ± S.D. (*error bars*) from three experiments; ***, $p < 0.001$, analyzed by Dunnett's multiple-comparison test). *B*, qPCR analysis for the expression of *Oct1*, *Elk1*, *c-Ets-1*, and *c-Rel* at differentiation days 0, 2, 3, and 4. Values are normalized to expression of *G3pdh* (mean ± S.D. from three experiments). *C*, qPCR analysis for expression of *Elk1*, *c-Ets-1*, and *c-Rel* in ES cells transfected with siRNAs against each transcription factor (*Elk1 si*, *c-Ets-1 si*, or *c-Rel si*) or control Luci siRNA. Values are normalized to expression of *G3pdh* (mean ± S.D. from three experiments; *, $p < 0.05$, analyzed by Dunnett's multiple-comparison test). *D*, Western blotting analysis for Elk-1, c-Ets-1, c-Rel, mouse INSC, and control α-tubulin proteins in ES cells transfected with siRNAs against each transcription factor or control Luci siRNA at differentiation days 0 and 2. *E and F*, ES cells were transfected with the indicated luciferase reporter plasmids together with the indicated siRNAs. Luciferase activities of each sample at differentiation days 0 and 2 are shown. Values are normalized to the activity of co-transfected *Renilla* luciferase (mean ± S.D. from three experiments; *, $p < 0.05$, analyzed by Dunnett's multiple-comparison test). *G*, ES cells were transfected with luciferase reporter plasmids containing the −5,066 to +200 genomic region with mutation of the putative c-Rel binding site together with control pRL-SV40 plasmid. Luciferase activity was measured at differentiation days 0 and 2. Values are normalized to the activity of co-transfected *Renilla* luciferase (mean ± S.D. from three experiments; ***, $p < 0.001$, analyzed by Dunnett's multiple-comparison test). *H*, ES cells were transfected with luciferase reporter plasmid containing the −5,066 to +200 genomic region. ChIP-qPCR analyses against c-Rel (*left*), Elk1 and c-Ets-1 (*right*), or control IgG were performed at differentiation day 2 by using primer pairs for amplifying the region between −5,066 and −4,712. The obtained qPCR values are normalized by input DNA. -Fold enrichment relative to IgG is shown (mean ± S.D. from three independent experiments; **, $p < 0.01$, analyzed by Dunnett's multiple-comparison test). *I*, ES cells were transfected with luciferase reporter plasmids containing the −5,066 to −4,712 genomic region together with control pRL-SV40 plasmid and treated with IKK inhibitor II (10 or 20 μM) or DMSO for 24 h. Luciferase activity was measured at differentiation days 0 and 2. Values are normalized to the activity of co-transfected *Renilla* luciferase (mean ± S.D. from three experiments; *, $p < 0.05$, analyzed by Dunnett's multiple-comparison test). *J*, qPCR analysis for expression of c-*Rel* and mouse *Insc* in ES cells transfected with c-Rel siRNA or control Luci siRNA at differentiation days 0 and 2. Values are normalized to the expression of *G3pdh* (mean ± S.D. from three experiments; *, $p < 0.05$, analyzed by Dunnett's multiple-comparison test). *K*, qPCR analysis for expression of *Oct4* in ES cells transfected with Oct4 siRNA or control Luci siRNA. Values are normalized to expression of *G3pdh* (mean ± S.D. from three experiments; *, $p < 0.05$, analyzed by Dunnett's multiple-comparison test) (*left*). Western blotting analysis for Oct4 and control α-tubulin proteins in ES cells transfected with Oct4 siRNA or control Luci siRNA at differentiation days 0 and 2 (*middle*). Shown are immunofluorescence images of Hoechst (*blue*), Oct4 (*green*), and Nanog (*red*) in mES cells transfected with Oct4 siRNAs or control Luci siRNA at differentiation days 0 and 2. *Scale bars*, 25 μm. *L*, ES cells were transfected with the indicated luciferase reporter plasmids together with siRNA against Oct4 or control Luci siRNA. Luciferase activities of each sample at differentiation days 0 and 2 are shown. Values are normalized to the activity of co-transfected *Renilla* luciferase (mean ± S.D. from three experiments; *, $p < 0.05$, analyzed by Dunnett's multiple-comparison test). *M*, qPCR analysis for the expression of *Nanog* and mouse *Insc* in ES cells transfected with Oct4 siRNA or control Luci siRNA at differentiation days 0 and 2. Values are normalized to the expression of *G3pdh* (mean ± S.D. from three experiments; *, $p < 0.05$, analyzed by Dunnett's multiple-comparison test).

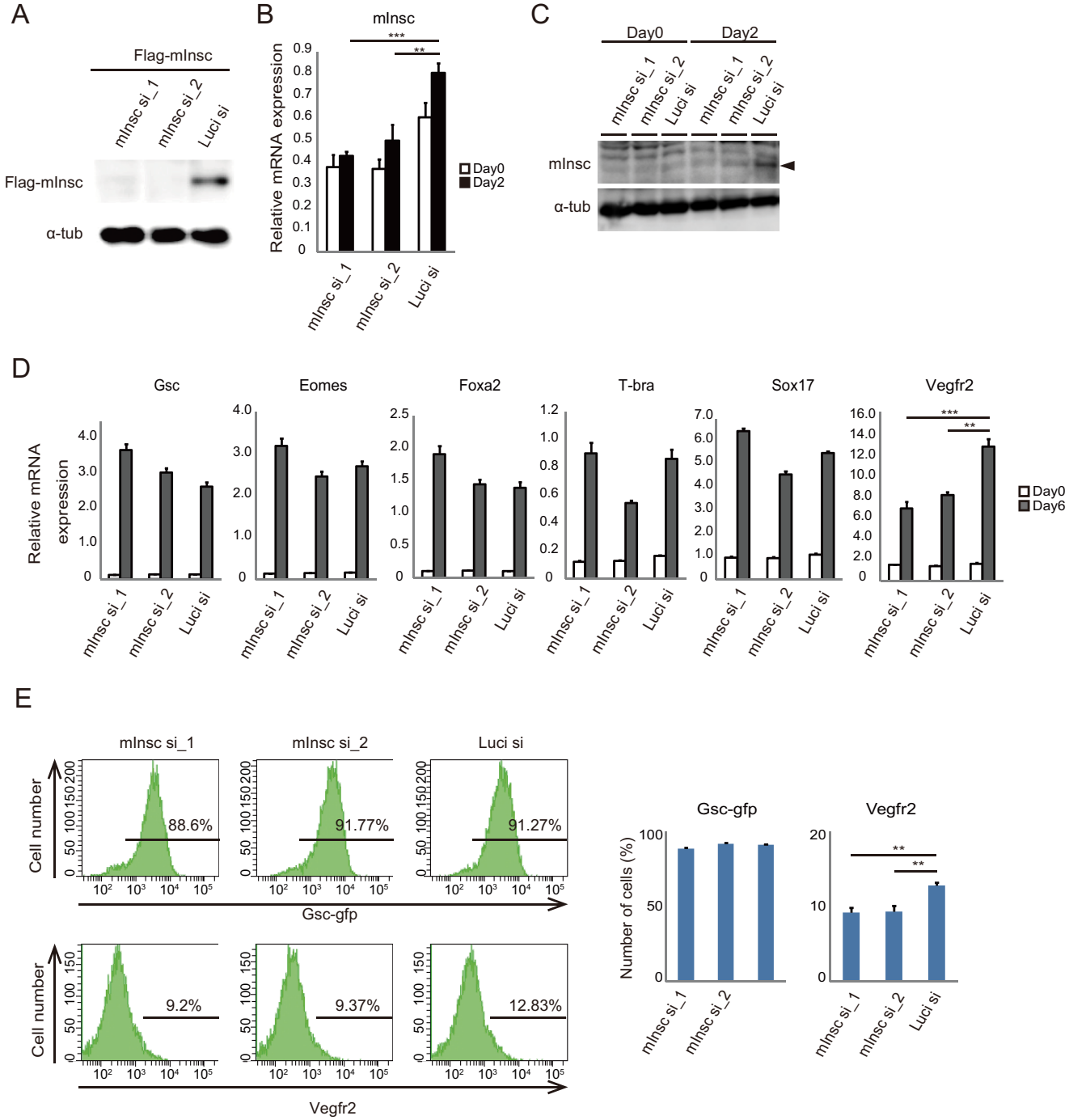

FIGURE 4. **Mouse INSC regulates mesoderm differentiation of ES cells.** *A*, Western blotting analysis of FLAG-mouse INSC and control α-tubulin proteins in HEK293T cells transfected with pENTR/pEF1a/FLAG-mouse INSC vector and mouse INSC siRNAs (*mInsc si_1* and *mInsc si_2*) or control Luci siRNA (*Luci si*). *B*, qPCR analysis for expression of mouse *Insc* in ES cells transfected with mouse INSC siRNAs or Luci siRNA at differentiation days 0 and 2. *C*, Western blotting analysis of mouse INSC and control α-tubulin proteins in ES cells transfected with mouse INSC siRNAs or Luci siRNA at differentiation days 0, 2, 3, and 4. *Arrowhead*, mouse INSC protein. *D*, qPCR analysis for expression of *Gsc*, *Eomes*, *Foxa2*, *T-bra*, *Sox17*, and *VEGFR-2* at differentiation days 0 and 6. In all qPCR analysis in *B* and *D*, values are normalized to the expression of *G3pdh* (mean ± S.D. (*error bars*) from three experiments; **, $p < 0.01$; ***, $p < 0.001$, analyzed by Dunnett's multiple-comparison test). *E*, FACS analysis for detecting Gsc-gfp (*left*, *top*) and VEGFR-2 (*left*, *bottom*) expression in ES cells transfected with mouse INSC siRNAs or Luci siRNA at differentiation day 6. The quantitative results are shown on the *right* (mean ± S.D. from three experiments; **, $p < 0.01$, analyzed by Dunnett's multiple-comparison test).

moter activity of the minimum DNA regulatory element in a dose-dependent manner (Fig. 3*I*) with only limited effects on cell survival and proliferation (data not shown), suggesting that NF-κB signaling is involved in the mouse *Insc* expression. Furthermore, siRNA-mediated knockdown of c-Rel suppressed expression levels of endogenous mouse *Insc* mRNA and protein (Fig. 3, *J* and *D*). These results demonstrate that mouse *Insc* transcription is regulated by c-Rel through binding to the 5-kb upstream region of the mouse *Insc* locus during mES cell differentiation into mesoderm and endoderm.

Although our used Match program of TRANSFAC® version 6.0 did not identify Oct4 as a candidate transcription factor that

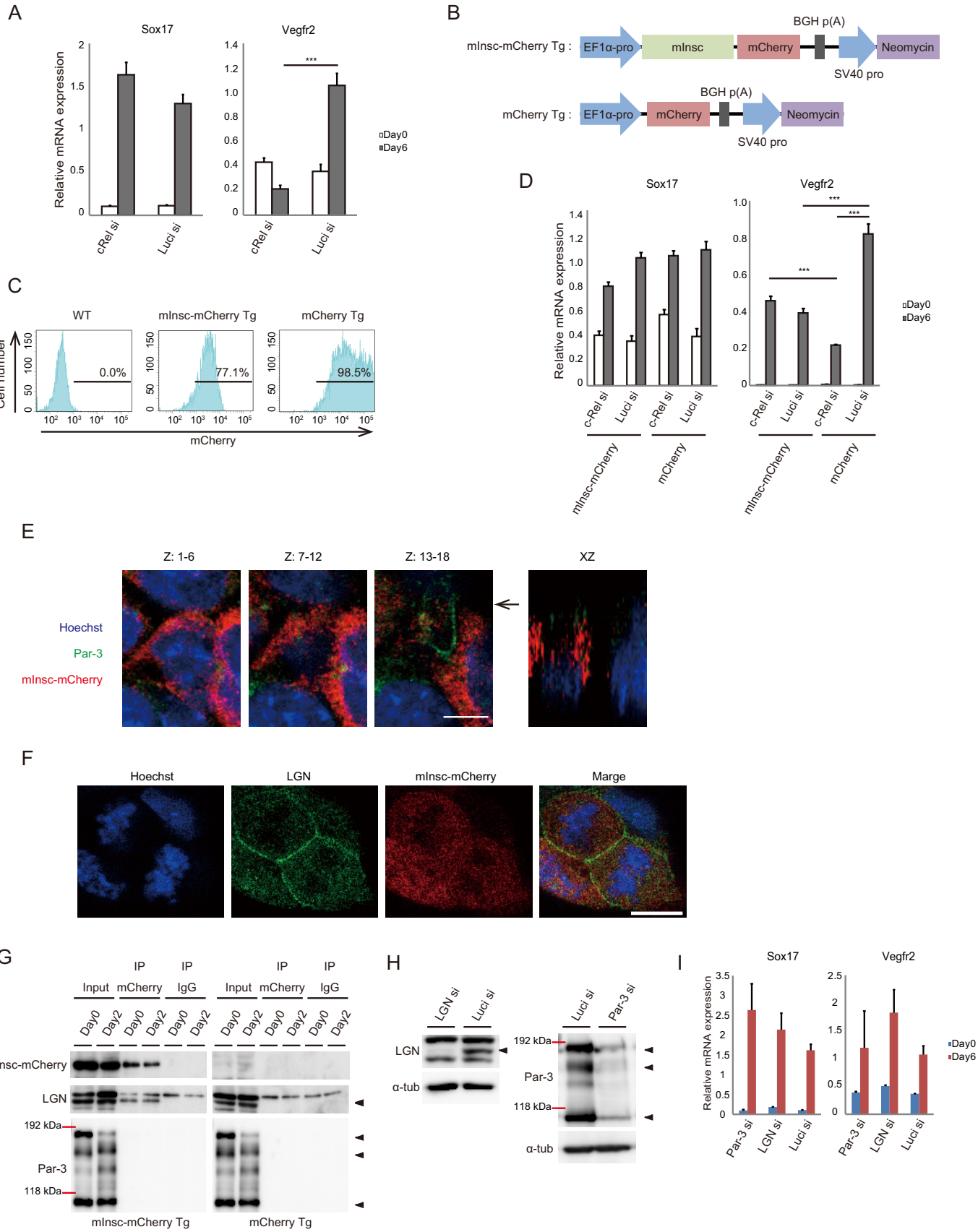
A
Sox17
Vegfr2
Relative mRNA expression
***
Day0
Day6
cRel si
Luci si
B
mInsc-mCherry Tg :
EF1α-pro
mInsc
mCherry
BGH p(A)
Neomycin
SV40 pro
mCherry Tg :
C
WT
mInsc-mCherry Tg
mCherry Tg
Cell number
0.0%
77.1%
98.5%
mCherry
D
Sox17
Vegfr2
Relative mRNA expression
c-Rel si
Luci si
mInsc-mCherry
mCherry
E
Z: 1-6
Z: 7-12
Z: 13-18
XZ
Hoechst
Par-3
mInsc-mCherry
F
Hoechst
LGN
mInsc-mCherry
Marge
G
IP
Input
mCherry
IgG
Day0
Day2
mInsc-mCherry
LGN
192 kDa
Par-3
118 kDa
mInsc-mCherry Tg
mCherry Tg
H
LGN si
Luci si
Par-3 si
LGN
α-tub
192 kDa
Par-3
118 kDa
I
Sox17
Vegfr2
Relative mRNA expression
Par-3 si
LGN si
Luci si
Day0
Day6

binds to the minimum transcription-promoting element (−5066 to −4712), the consensus binding sequence of Oct4 is the same as that of Oct1 (49). Oct4 protein is enriched in ES cells, raising the possibility that Oct4 regulates mouse *Insc* expression. Then we depleted Oct4 by siRNA to assess its contribution to mouse *Insc* expression during differentiation. Down-regulation of *Oct4* mRNA and protein by the used siRNA was confirmed by qPCR, immunoblotting, and immunostaining (Fig. 3*K*). Interestingly, Oct4 knockdown significantly decreased promoter activity of both the minimum DNA regulatory element and the base −5382 upstream region of the mouse *Insc* locus (Fig. 3*L*). In addition, the expression level of endogenous mouse *Insc* mRNA was decreased in the Oct4-depleted cells (Fig. 3*M*). These results support the idea that, in addition to c-Rel, Oct4 regulates mouse *Insc* expression during ES cell differentiation into mesoderm and endoderm. However, because Oct4 is necessary for ES cell pluripotency (50), depletion of Oct4 could alter cell properties of ES cells. Consistently, we observed decreased expression of pluripotent gene *Nanog* mRNA and protein in the Oct4-depleted cells at differentiation day 0 (Fig. 3, *K* and *M*). Therefore, we cannot exclude the possibility that the down-regulation of the promoter activity and the expression level of mouse *Insc* in the Oct4-depleted cells are indirect effects of the changes in cell property.

Mouse INSC Regulates Mesoderm Fate Decisions of ES Cells—Next, we attempted to investigate whether mouse INSC plays a role in cell fate determination of ES cells into mesendoderm, mesoderm, or endoderm. To examine this possibility, we knocked down mouse INSC protein by RNAi using two independent siRNAs. These siRNAs effectively decreased the protein levels of ectopically expressed FLAG-tagged mouse INSC in HEK293T cells (Fig. 4*A*) as well as the levels of endogenous mouse *Insc* mRNA and protein in ES cells differentiating into mesendoderm (Fig. 4, *B* and *C*). Knockdown of mouse *Insc* significantly suppressed expression of VEGFR-2, whereas expression levels of Gsc, Eomes, FoxA2, T-bra, and Sox17 were similar to those in control luciferase siRNA-transfected cells at differentiation day 6 (Fig. 4*D*). Additionally, flow cytometric analysis indicated a decrease in the population of VEGFR-2-positive cells at differentiation day 6, when the cells were depleted of mouse INSC, whereas the population of Gsc-GFP-positive cells remained constant (Fig. 4*E*). These results indicate that mouse INSC regulates mesoderm differentiation of ES cells.

c-Rel Regulates Mesoderm Fate Decisions of ES Cells through Mouse INSC—Similar to mouse INSC, we found that siRNA-mediated knockdown of c-Rel significantly suppressed the expression of *VEGFR-2*, whereas the expression level of *Sox17* was only increased slightly (Fig. 5*A*), indicating the requirement of c-Rel in mesoderm differentiation. Our data showed that expression of mouse *Insc* was dependent on c-Rel (Fig. 3, *D* and *I*). Then we examined whether c-Rel regulates mesoderm differentiation of ES cells through mouse *Insc*. To address this issue, we established ES cell lines with constituently expressed mouse INSC-mCherry or control mCherry driven by the EF1α promoter (mouse INSC-mCherry and mCherry Tg ES cells, respectively) (Fig. 5, *B* and *C*). Notably, mouse INSC-mCherry Tg ES cells displayed a decrease in the expression of *VEGFR-2* compared with mCherry Tg ES cells at differentiation day 6, whereas expression of Sox17 was comparable (Fig. 5*D*). Similar to knockdown of mouse INSC, these results indicated that overexpression of mouse INSC suppresses mesoderm differentiation of ES cells. As expected, siRNA-mediated knockdown of c-Rel in mCherry Tg ES cells significantly suppressed expression of *VEGFR-2* at day 6 with no detectable change in the expression level of *Sox17* in mCherry Tg ES cells (Fig. 5*D*). However, knockdown of c-Rel did not suppress expression of *VEGFR-2* in mouse INSC-mCherry Tg ES cells (Fig. 5*D*). Instead, the expression level of *VEGFR-2* was significantly higher in mouse INSC-mCherry Tg ES cells than in mCherry Tg ES cells when the cells were depleted of c-Rel (Fig. 5*D*), indicating that overexpression of mouse INSC rescued the mesoderm-suppressed phenotype induced by knockdown of c-Rel. Taken together, our data support a model in which c-Rel regulates mesoderm differentiation of ES cells by promoting the expression of mouse INSC.

Insc is a well known regulator of asymmetric cell division, raising the possibility that asymmetric cell division occurs during mES cell differentiation into mesoderm and endoderm, in which mouse INSC might play a vital role. However, in differentiating mES cells, our immunohistochemical analysis showed mCherry-mouse INSC and endogenous mouse INSC protein in the cytoplasm and no evidence of asymmetric staining patterns (Fig. 5, *E* and *F*), although we detected polarized apical localization of Par-3 in interphase cells as well as polarized cortical localization of LGN in mitotic cells (Fig. 5, *E* and *F*). We found an association of mouse INSC with LGN, but not Par-3, in immunoprecipitation analyses (Fig. 5*G*). Furthermore, differentiation of ES cells into mesoderm and endoderm was only

FIGURE 5. **c-Rel regulates mesoderm differentiation of ES cells through mouse INSC.** *A*, qPCR analysis for expression of *Sox17* and *Vegfr2* in ES cells transfected with c-Rel siRNA or control Luci siRNA at differentiation days 0 and 6. *B*, schematic diagram of the constructs used for establishing mouse INSC-mCherry Tg ES cell lines and mCherry Tg ES cell lines. *C*, FACS analysis for detecting mCherry expression in mouse INSC-mCherry Tg (*middle*) and mCherry Tg (*right*) ES cell lines and control ES cells (*left*, *WT*). *D*, qPCR analysis for expression of *Sox17* and *Vegfr2* in mouse INSC-mCherry Tg ES cell lines or mCherry Tg ES cell lines transfected with c-Rel siRNA or control Luci siRNA at differentiation days 0 and 6. *E*, immunofluorescence images of mouse INSC-mCherry Tg ES cells at differentiation day 2. Z-stack images of Hoechst (*blue*), Par-3 (*green*), and mouse INSC-mCherry (*red*) are shown in the *left panels*. The *x-z* projection image on the plane indicated by an *arrow* is shown on the *right*. *Scale bar*, 10 μm. *F*, immunofluorescence images of Hoechst (*blue*), LGN (*green*), and mouse INSC-mCherry (*red*) of the mouse INSC-mCherry Tg ES cells at differentiation day 2. *Scale bar*, 10 μm. *G*, co-immunoprecipitation analysis for mouse INSC-mCherry and LGN or Par-3. Total lysates were prepared from the mouse INSC-mCherry Tg ES cells or mCherry Tg ES cells at differentiation day 0 or 2, subjected to immunoprecipitation with anti-mCherry antibodies, and analyzed by Western blotting with anti-Ds-Red (which recognizes mCherry), anti-LGN, and anti-Par-3 antibodies. *H*, Western blotting analysis of LGN (*left*), Par-3 (*right*), and control α-tubulin in ES cells transfected with either LGN siRNA, Par-3 siRNA, or Luci siRNA. *Arrowheads*, LGN protein and three variants of Par-3 proteins. *I*, qPCR analysis for expression of *Sox17* and *Vegfr2* in ES cells transfected with either LGN siRNA, Par-3 siRNA, or control Luci siRNA at differentiation days 0 and 6. In qPCR analysis in *A*, *D*, and *I*, values are normalized to expression of *G3pdh* (mean ± S.D. (*error bars*) from three experiments; ***, $p < 0.001$, analyzed by Dunnett's multiple-comparison test in *A* and *I* or Tukey's multiple-comparison test in *D*).

partially affected by siRNA-mediated knockdown of LGN or Par-3 (Fig. 5, *H* and *I*). These observations favor a model in which mouse INSC regulates mesoderm differentiation of ES cells by a mechanism that is independent of asymmetric cell division.

Discussion

The regulatory mechanisms underlying mouse *Insc* expression have been largely unknown despite its critical role in cell fate determination of various cell types in mammals. Here, we identified a minimum promoter element that drives mouse *Insc* expression in differentiating mES cells. In general, TATA elements (located ~25–30 bases upstream of the TSS) and an initiator motif (a pyrimidine-rich sequence encompassing the TSS) are important for eukaryotic gene expression (51–53). Inconsistently, however, our data showed that deletion of the region between bases −631 and −1 upstream of the mouse *Insc* TSS only partially decreased mouse *Insc* expression. In addition, no promoter activity was detected in a series of constructs in the region between −4,382 and −382. Therefore, the 4,382-base upstream region of the TSS is expendable for mouse *Insc* expression. Because deletion of the region between −4,046 and −1 drastically increased promoter activity in both undifferentiated and differentiated cells, we speculate that this region harbors suppressor or structural elements that suppress mouse *Insc* expression.

We found a minimum promoter element within a region between −5,066 and −4,712 bases upstream of the mouse *Insc* gene locus and identified a key transcription factor, c-Rel, which binds to the minimum promoter and drives mouse *Insc* expression in ES cells. Involvement of nuclear factor-κB (NF-κB) signaling in mES cell differentiation (54, 55) is consistent with these results. The relationship between c-Rel and mouse INSC is supported by previous reports that revealed functions of c-Rel in cell proliferation and differentiation of neural progenitors and epidermal cells (56, 57), whereby mouse INSC regulates their cell fate (28–31). This observation suggests that c-Rel regulates cell fate determination by promoting mouse *Insc* expression. Our finding that the reduction of mesodermal cells induced by loss of c-Rel is rescued by mouse INSC overexpression further supports this model. However, it is unlikely that c-Rel is the sole regulator for mouse *Insc* expression. Our data showing that the region between −5,382 and −4,712 bases upstream has higher promoter activity than the minimum promoter implicates a co-regulatory element that drives mouse *Insc* expression within the region between −5,382 and −5,066, although this region alone is not sufficient for promoter activity. While we were preparing this manuscript, Ballard *et al.* (58) reported that SNAL1 enhances mouse *Insc* expression in mammary stem cells. They used a 224-bp DNA fragment containing the upstream region of human *Inscuteable* for luciferase assays. This sequence is not conserved in mice (data not shown). However, we found a SNAIL1 consensus-binding sequence, TCACA, within the co-regulatory region at 5,195–5,191 bases upstream of the mouse *Insc* gene locus. Therefore, SNAIL1 might function as a co-regulator that enhances c-Rel-mediated mouse *Insc* transcription in mES cells. In addition, our used Match program of TRANSFAC® version 6.0 also identified the Evi1 consensus-binding sequence, AGAGA, at bases 5,235 to 5,231 upstream of the mouse *Insc* gene locus. Moreover, our finding that mutation of the binding sites for Oct1, Elk1, or c-Ets-1 results in loss of promoter activity further supports the concept of a co-regulatory mechanism for mouse *Insc* transcription. It appears likely that these co-regulators function in a complementary manner, because knockdown of Elk1 alone did not suppress mouse *Insc* expression, despite its association with the minimum promoter. We speculate that the regulatory mechanism for mouse *Insc* transcription varies, depending on the cell type or differentiation conditions. The underlying mechanisms should be elucidated in future studies.

The function of Insc in asymmetric cell division is well established, and its overexpression alters the balance between symmetric/asymmetric cell division. Although asymmetric cell division during ES cell differentiation has received little attention, recent studies have demonstrated that Wnt protein-immobilized beads attached to the cell surface induce asymmetric division of mES cells with mitotic spindles aligned along a Wnt bead-induced polarity axis (59). Additionally, in defined culture conditions, mES cells have been differentiated into bipotent mesendoderm cells capable of giving rise to both endoderm and mesoderm lineages (36, 37). These data raise the possibility of Insc-dependent asymmetric cell division occurring during mES cell differentiation into mesoderm and endoderm. However, our results provided no evidence for asymmetric staining patterns of mouse INSC-mCherry protein or involvement of asymmetric cell division in the mesoderm cell fate decision of mES cells. These observations are consistent with a previous study showing that Staufen, an Insc-binding protein that functions in mRNA processing and basal localization of Pros mRNA in *Drosophila* neuroblasts, regulates mES cell differentiation without displaying an asymmetric distribution (60). Thus, one potential model is that mouse INSC regulates mesoderm cell fate through Staufen. However, we cannot exclude the possibility that asymmetric cell division occurs only in a very small population of differentiating ES cells. Further studies are necessary to elucidate how mouse INSC specifies the mesoderm cell lineage of differentiating ES cells.

c-Rel, a member of the NF-κB transcription factor family (61–63), regulates gene expression of various cytokines and transcription factors important for proper functioning of B cells, T cells, macrophages, and dendritic cells (62–65). Importantly, c-Rel also regulates development of T regulatory cells, Th1 cells, and Th17 cells (64–67). Because our results show that mouse *Insc* gene expression is regulated by c-Rel, it would be interesting to investigate a potential c-Rel/mouse INSC axis capable of directing T cell development.

Author Contributions—R. I., H. S., and F. T. designed the research; R. I., and S. Kozuki, and S. Kamakura performed the experiments; R. I. and F. T. analyzed data; and R. I and F. T. wrote the paper.

Acknowledgment—We thank T. Era (Kumamoto University) for $Gsc^{gfp/+}$ *ES cells.*

References

1. Kraut, R., and Campos-Ortega, J. A. (1996) Inscuteable, a neural precursor gene of *Drosophila*, encodes a candidate for a cytoskeleton adaptor protein. *Dev. Biol.* **174,** 65–81
2. Kraut, R., Chia, W., Jan, L. Y., Jan, Y. N., and Knoblich, J. A. (1996) Role of inscuteable in orienting asymmetric cell divisions in *Drosophila*. *Nature* **383,** 50–55
3. Knoblich, J. A. (1997) Mechanisms of asymmetric cell division during animal development. *Curr. Opin. Cell Biol.* **9,** 833–841
4. Siller, K. H., and Doe, C. Q. (2009) Spindle orientation during asymmetric cell division. *Nat. Cell Biol.* **11,** 365–374
5. Lu, B., Jan, L., and Jan, Y. N. (2000) Control of cell divisions in the nervous system: symmetry and asymmetry. *Annu. Rev. Neurosci.* **23,** 531–556
6. Neumüller, R. A., and Knoblich, J. A. (2009) Dividing cellular asymmetry: asymmetric cell division and its implications for stem cells and cancer. *Genes Dev.* **23,** 2675–2699
7. Ikeshima-Kataoka, H., Skeath, J. B., Nabeshima, Y., and Doe, C. Q., and Matsuzaki F. (1997) Miranda directs Prospero to a daughter cell during *Drosophila* asymmetric divisions. *Nature* **390,** 625–629
8. Shen, C. P., Jan, L. Y., and Jan, Y. N. (1997) Miranda is required for the asymmetric localization of Prospero during mitosis in *Drosophila*. *Cell* **90,** 449–458
9. Doe, C. Q., Chu-LaGraff, Q., Wright, D. M., and Scott, M. P. (1991) The prospero gene specifies cell fates in the *Drosophila* central nervous system. *Cell* **65,** 451–464
10. Hirata, J., Nakagoshi, H., Nabeshima, Y., and Matsuzaki, F. (1995) Asymmetric segregation of the homeodomain protein Prospero during *Drosophila* development. *Nature* **377,** 627–630
11. Knoblich, J. A., Jan, L. Y., and Jan, Y. N. (1995) Asymmetric segregation of Numb and Prospero during cell division. *Nature* **377,** 624–627
12. Matsuzaki, F., Koizumi, K., Hama, C., Yoshioka, T., and Nabeshima, Y. (1992) Cloning of the *Drosophila* prospero gene and its expression in ganglion mother cells. *Biochem. Biophys. Res. Commun.* **182,** 1326–1332
13. Spana, E. P., and Doe, C. Q. (1995) The prospero transcription factor is asymmetrically localized to the cell cortex during neuroblast mitosis in *Drosophila*. *Development* **121,** 3187–3195
14. Vaessin, H., Grell, E., Wolff, E., Bier, E., Jan, L. Y., and Jan, Y. N. (1991) prospero is expressed in neuronal precursors and encodes a nuclear protein that is involved in the control of axonal outgrowth in *Drosophila*. *Cell* **67,** 941–953
15. Bello, B., Reichert, H., and Hirth, F. (2006) The brain tumor gene negatively regulates neural progenitor cell proliferation in the larval central brain of *Drosophila*. *Development* **133,** 2639–2648
16. Betschinger, J., Mechtler, K., and Knoblich, J. A. (2006) Asymmetric segregation of the tumor suppressor brat regulates self-renewal in *Drosophila* neural stem cells. *Cell* **124,** 1241–1253
17. Lee, C. Y., Wilkinson, B. D., Siegrist, S. E., Wharton, R. P., and Doe, C. Q. (2006) Brat is a Miranda cargo protein that promotes neuronal differentiation and inhibits neuroblast self-renewal. *Dev. Cell.* **10,** 441–449
18. Rhyu, M. S., Jan, L. Y., and Jan, Y. N. (1994) Asymmetric distribution of numb protein during division of the sensory organ precursor cell confers distinct fates to daughter cells. *Cell* **76,** 477–491
19. Spana, E. P., Kopczynski, C., Goodman, C. S., Doe, C. Q. (1995) Asymmetric localization of numb autonomously determines sibling neuron identity in the *Drosophila* CNS. *Development* **121,** 3489–3494
20. Uemura, T., Shepherd, S., Ackerman, L., Jan, L. Y., and Jan, Y. N. (1989) numb, a gene required in determination of cell fate during sensory organ formation in *Drosophila* embryos. *Cell* **58,** 349–360
21. Buescher, M., Yeo, S. L., Udolph, G., Zavortink, M., Yang, X., Tear, G., and Chia, W. (1998) Binary sibling neuronal cell fate decisions in the *Drosophila* embryonic central nervous system are nonstochastic and require inscuteable-mediated asymmetry of ganglion mother cells. *Genes Dev.* **12,** 1858–1870
22. Skeath, J. B., and Doe, C. Q. (1998) Sanpodo and Notch act in opposition to Numb to distinguish sibling neuron fates in the *Drosophila* CNS. *Development* **125,** 1857–1865
23. Yu, F., Morin, X., Cai, Y., Yang, X., and Chia, W. (2000) Analysis of partner of inscuteable, a novel player of *Drosophila* asymmetric divisions, reveals two distinct steps in inscuteable apical localization. *Cell* **100,** 399–409
24. Parmentier, M. L., Woods, D., Greig, S., Phan, P. G., Radovic, A., Bryant, P., O'Kane, C. J. (2000) Rapsynoid/partner of inscuteable controls asymmetric division of larval neuroblasts in *Drosophila*. *J. Neurosci.* **20,** RC84
25. Schaefer, M., Shevchenko, A., Shevchenko, A., and Knoblich, J. A. (2000) A protein complex containing Inscuteable and the Gα-binding protein Pins orients asymmetric cell divisions in *Drosophila*. *Curr. Biol.* **10,** 353–362
26. Wang, C., Li, S., Januschke, J., Rossi, F., Izumi, Y., Garcia-Alvarez, G., Gwee, S. S., Soon, S. B., Sidhu, H. K., Yu, F., Matsuzaki, F., Gonzalez, C., and Wang, H. (2011) An ana2/ctp/mud complex regulates spindle orientation in *Drosophila* neuroblasts. *Dev. Cell.* **21,** 520–533
27. Zigman, M., Cayouette, M., Charalambous, C., Schleiffer, A., Hoeller, O., Dunican, D., McCudden, C. R., Firnberg, N., Barres, B. A., Siderovski, D. P., and Knoblich, J. A. (2005) Mammalian inscuteable regulates spindle orientation and cell fate in the developing retina. *Neuron* **48,** 539–545
28. Postiglione, M. P., Jüschke, C., Xie, Y., Haas, G. A., Charalambous, C., and Knoblich, J. A. (2011) Mouse inscuteable induces apical-basal spindle orientation to facilitate intermediate progenitor generation in the developing neocortex. *Neuron* **72,** 269–284
29. Lechler, T., and Fuchs, E. (2005) Asymmetric cell divisions promote stratification and differentiation of mammalian skin. *Nature* **437,** 275–280
30. Williams, S. E., Beronja, S., Pasolli, H. A., and Fuchs, E. (2011) Asymmetric cell divisions promote Notch-dependent epidermal differentiation. *Nature* **470,** 353–358
31. Williams, S. E., Ratliff, L. A., Postiglione, M. P., Knoblich, J. A., and Fuchs E. (2014) Par3-mInsc and $G\alpha_{i3}$ cooperate to promote oriented epidermal cell divisions through LGN. *Nat. Cell Biol.* **16,** 758–769
32. Evans, M. J., and Kaufman, M. H. (1981) Establishment in culture of pluripotential cells from mouse embryos. *Nature* **292,** 154–156
33. Martin, G. R. (1981) Isolation of a pluripotent cell line from early mouse embryos cultured in medium conditioned by teratocarcinoma stem cells. *Proc. Natl. Acad. Sci. U.S.A.* **78,** 7634–7638
34. Doetschman, T. C., Eistetter, H., Katz, M., Schmidt, W., and Kemler, R. (1985) The *in vitro* development of blastocyst-derived embryonic stem cell lines: formation of visceral yolk sac, blood islands and myocardium. *J. Embryol. Exp. Morphol.* **87,** 27–45
35. Nishikawa, S., Jakt, L. M., and Era, T. (2007) Embryonic stem-cell culture as a tool for developmental cell biology. *Nat. Rev. Mol. Cell. Biol.* **8,** 502–507
36. Tada, S., Era, T., Furusawa, C., Sakurai, H., Nishikawa, S., Kinoshita, M., Nakao, K., Chiba, T., and Nishikawa, S. (2005) Characterization of mesendoderm: a diverging point of the definitive endoderm and mesoderm in embryonic stem cell differentiation culture. *Development* **132,** 4363–4374
37. Yasunaga, M., Tada, S., Torikai-Nishikawa, S., Nakano, Y., Okada, M., Jakt, L. M., Nishikawa, S., Chiba, T., Era, T., and Nishikawa, S. (2005) Induction and monitoring of definitive and visceral endoderm differentiation of mouse ES cells. *Nat. Biotechnol.* **23,** 1542–1550
38. Kamakura, S., Nomura, M., Hayase, J., Iwakiri, Y., Nishikimi, A., Takayanagi, R., Fukui, Y., and Sumimoto, H. (2013) The cell polarity protein mInsc regulates neutrophil chemotaxis via a noncanonical G protein signaling pathway. *Dev. Cell.* **26,** 292–302
39. Kataoka, H., Takakura, N., Nishikawa, S., Tsuchida, K., Kodama, H., Kunisada, T., Risau, W., Kita, T., and Nishikawa, S. I. (1997) Expressions of PDGF receptor α, c-Kit and Flk1 genes clustering in mouse chromosome 5 define distinct subsets of nascent mesodermal cells. *Dev. Growth Differ.* **39,** 729–740
40. Kanai-Azuma, M., Kanai, Y., Gad, J. M., Tajima, Y., Taya, C., Kurohmaru, M., Sanai, Y., Yonekawa, H., Yazaki, K., Tam, P. P., and Hayashi, Y. (2002) Depletion of definitive gut endoderm in Sox17-null mutant mice. *Development* **129,** 2367–2379
41. Tam, P. P., Kanai-Azuma, M., and Kanai, Y. (2003) Early endoderm development in vertebrates: lineage differentiation and morphogenetic function. *Curr. Opin. Genet. Dev.* **13,** 393–400
42. Izumi, N., Era, T., Akimaru, H., Yasunaga, M., and Nishikawa, S. (2007) Dissecting the molecular hierarchy for mesendoderm differentiation through a combination of embryonic stem cell culture and RNA interference. *Stem Cells* **25,** 1664–1674

43. van den Ameele, J., Tiberi, L., Bondue, A., Paulissen, C., Herpoel, A., Iacovino, M., Kyba, M., Blanpain, C., and Vanderhaeghen, P. (2012) Eomesodermin induces Mesp1 expression and cardiac differentiation from embryonic stem cells in the absence of Activin. *EMBO Rep.* **13,** 355–362
44. Ang, S. L., Wierda, A., Wong, D., Stevens, K. A., Cascio, S., Rossant, J., and Zaret, K. S. (1993) The formation and maintenance of the definitive endoderm lineage in the mouse: involvement of HNF3/forkhead proteins. *Development* **119,** 1301–1315
45. Era, T., Izumi, N., Hayashi, M., Tada, S., Nishikawa, S., and Nishikawa, S. (2008) Multiple mesoderm subsets give rise to endothelial cells, whereas hematopoietic cells are differentiated only from a restricted subset in embryonic stem cell differentiation culture. *Stem Cells* **26,** 401–411
46. Niwa, H., Ogawa, K., Shimosato, D., and Adachi, K. (2009) A parallel circuit of LIF signalling pathways maintains pluripotency of mouse ES cells. *Nature* **460,** 118–122
47. Thomson, M., Liu, S. J., Zou, L. N., Smith, Z., Meissner, A., and Ramanathan, S. (2011) Pluripotency factors in embryonic stem cells regulate differentiation into germ layers. *Cell* **145,** 875–889
48. Kobori, M., Yang, Z., Gong, D., Heissmeyer, V., Zhu, H., Jung, Y. K., Gakidis, M. A., Rao, A., Sekine, T., Ikegami, F., Yuan, C., and Yuan, J. (2004) Wedelolactone suppresses LPS-induced caspase-11 expression by directly inhibiting the IKK complex. *Cell Death Differ.* **11,** 123–130
49. Schöler, H. R., Balling, R., Hatzopoulos, A. K., Suzuki, N., and Gruss, P. (1989) Octamer binding proteins confer transcriptional activity in early mouse embryogenesis. *EMBO J.* **8,** 2551–2557
50. Niwa, H., Miyazaki, J., and Smith, A. G. (2000) Quantitative expression of Oct-3/4 defines differentiation, dedifferentiation or self-renewal of ES cells. *Nat. Genet.* **24,** 372–376
51. Nakajima, N., Horikoshi, M., and Roeder, R. G. (1988) Factors involved in specific transcription by mammalian RNA polymerase II: purification, genetic specificity, and TATA box-promoter interactions of TFIID. *Mol. Cell. Biol.* **8,** 4028–4040
52. Parker, C. S., and Topol, J. (1984) A *Drosophila* RNA polymerase II transcription factor contains a promoter-region-specific DNA-binding activity. *Cell* **36,** 357–369
53. Weis, L., and Reinberg, D. (1992) Transcription by RNA polymerase II: initiator-directed formation of transcription-competent complexes. *FASEB J.* **6,** 3300–3309
54. Torres, J., and Watt, F. M. (2008) Nanog maintains pluripotency of mouse embryonic stem cells by inhibiting NFκB and cooperating with Stat3. *Nat. Cell Biol.* **10,** 194–201
55. Kim, Y. E., Kang, H. B., Park, J. A., Nam, K. H., Kwon, H. J., and Lee, Y. (2008) Upregulation of NF-κB upon differentiation of mouse embryonic stem cells. *BMB Rep.* **41,** 705–709
56. Young, K. M., Bartlett, P. F., and Coulson, E. J. (2006) Neural progenitor number is regulated by nuclear factor-κB p65 and p50 subunit-dependent proliferation rather than cell survival. *J. Neurosci. Res.* **83,** 39–49
57. Fullard, N., Moles, A., O'Reilly, S., van Laar, J. M., Faini, D., Diboll, J., Reynolds, N. J., Mann, D. A., Reichelt, J., and Oakley, F. (2013) The c-Rel subunit of NF-κB regulates epidermal homeostasis and promotes skin fibrosis in mice. *Am. J. Pathol.* **182,** 2109–2120
58. Ballard, M. S., Zhu, A., Iwai, N., Stensrud, M., Mapps, A., Postiglione, M. P., Knoblich, J. A., and Hinck, L. (2015) Mammary stem cell self-renewal is regulated by Slit2/Robo1 signaling through SNAI1 and mINSC. *Cell Rep.* **13,** 290–301
59. Habib, S. J., Chen, B. C., Tsai, F. C., Anastassiadis, K., Meyer, T., Betzig, E., and Nusse, R. (2013) A localized Wnt signal orients asymmetric stem cell division *in vitro*. *Science* **339,** 1445–1448
60. Li, P., Yang, X., Wasser, M., Cai, Y., and Chia, W. (1997) Inscuteable and Staufen mediate asymmetric localization and segregation of prospero RNA during *Drosophila* neuroblast cell divisions. *Cell.* **90,** 437–447
61. Gilmore, T. D., and Gerondakis, S. (2011) The c-Rel transcription factor in development and disease. *Genes Cancer* **2,** 695–711
62. Hayden, M. S., and Ghosh, S. (2004) Signaling to NF-κB. *Genes Dev.* **18,** 2195–2224
63. Perkins N. D. (2007) Integrating cell-signalling pathways with NF-κB and IKK function. *Nat. Rev. Mol. Cell Biol.* **8,** 49–62
64. Liou, H. C., and Hsia, C. Y. (2003) Distinctions between c-Rel and other NF-κB proteins in immunity and disease. *Bioessays* **8,** 767–780
65. Isomura, I., Palmer, S., Grumont, R. J., Bunting, K., Hoyne, G., Wilkinson, N., Banerjee, A., Proietto, A., Gugasyan, R., Wu, L., Li, W., McNally, A., Steptoe, R. J., Thomas, R., Shannon, M. F., and Gerondakis, S. (2009) c-Rel is required for the development of thymic $Foxp3^+$ CD4 regulatory T cells. *J. Exp. Med.* **206,** 3001–3014
66. Hilliard, B. A., Mason, N., Xu, L., Sun, J., Lamhamedi-Cherradi, S. E., Liou, H. C., Hunter, C., and Chen, Y. H. (2002) Critical roles of c-Rel in autoimmune inflammation and helper T cell differentiation. *J. Clin. Invest.* **110,** 843–850
67. Chen, G., Hardy, K., Pagler, E., Ma, L., Lee, S., Gerondakis, S., Daley, S., and Shannon, M. F. (2011) The NF-κB transcription factor c-Rel is required for Th17 effector cell development in experimental autoimmune encephalomyelitis. *J. Immunol.* **187,** 4483–4491